

SPARK: Igniting Communication-Efficient Decentralized Learning via Stage-wise Projected NTK and Accelerated Regularization

Li Xia¹

Abstract

Decentralized federated learning (DFL) enables collaborative model training without a central server, but faces challenges from statistical heterogeneity. Recent NTK-based methods achieve faster convergence than existing DFL approaches, yet transmitting full Jacobian matrices creates prohibitive communication overhead for bandwidth-constrained edge networks. We propose SPARK, integrating random projection-based Jacobian compression, stage-wise annealed distillation, and Nesterov momentum acceleration to address this fundamental trade-off. SPARK compresses Jacobians via random projections while preserving essential spectral properties. Stage-wise annealed distillation counteracts compression noise by transitioning from pure NTK evolution to neighbor-regularized learning. Nesterov momentum enables stable gradient accumulation through distillation smoothing. Our method achieves 98.7% communication reduction while maintaining convergence speed and surpassing baseline accuracy across heterogeneity levels. With momentum, SPARK reaches target performance 3 times faster than state-of-the-art methods, establishing new benchmarks for communication-efficient decentralized learning in bandwidth-limited environments.

1. Introduction

Federated learning (FL) is a machine learning paradigm in which multiple clients train a global model without explicit communication of training data. In the popular federated averaging (FedAvg) algorithm (McMahan et al., 2017), clients perform multiple rounds of stochastic gradient descent (SGD) on local data, then send updated weight vectors to a central server for aggregation. As FL gains popularity,

numerous improvements have addressed challenges including communication efficiency, heterogeneous data distributions, and security concerns (Konečný et al., 2016; Li et al., 2020; Zhu et al., 2019). To handle performance degradation caused by data heterogeneity, many works have proposed mitigation strategies (Karimireddy et al., 2020; Li et al., 2020). Notably, some researchers have introduced the neural tangent kernel (NTK), replacing SGD to improve model convergence (Yu et al., 2022; Yue et al., 2022).

Despite these advancements, the centralized nature of traditional FL introduces possibilities for client data leakage, computational bottlenecks at the server, and high communication bandwidth demand (Kairouz et al., 2021). Decentralized federated learning (DFL) has been proposed as a solution (Marfoq et al., 2023). In DFL, clients communicate along an undirected graph, where each node represents a client and each edge represents a communication channel. While DFL addresses issues inherent to centralized FL, both frameworks grapple with statistical heterogeneity across clients. Although mixing data on a central server could resolve this issue, transmitting raw training data introduces privacy concerns, making FL and DFL good candidates to address this challenge (Philippenko & Dieuleveut, 2023).

Recent work has extended the NTK paradigm to decentralized settings. The NTK-DFL framework (Thompson et al., 2025) demonstrates that transmitting Jacobian matrices rather than weight vectors enables more expressive updates, achieving significantly faster convergence than existing DFL approaches in heterogeneous settings. However, this expressiveness comes at a significant cost: communication overhead. For typical edge models, transmitting Jacobians requires substantially more bandwidth than transmitting weight vectors. In resource-constrained edge environments such as IoT networks operating over LoRaWAN, 4G LTE, or satellite links, this order-of-magnitude increase in communication volume renders NTK-DFL impractical for deployment (Zhong & Nie, 2024; Sodiya et al., 2024).

This paper focuses on the following research question: Can we retain the convergence speed and robustness of NTK-based decentralized learning while drastically reducing communication overhead to levels viable for bandwidth-limited edge networks? Existing communication compression ap-

¹Key Laboratory of Ethnic Language Intelligent Analysis and Security Governance of MOE, Minzu University of China, Beijing, China. Correspondence to: Li Xia <xiali@muc.edu.cn>.

proaches, such as gradient quantization (Alistarh et al., 2017), sparsification (Lin et al., 2018), and low-rank factorization (Vogels et al., 2019), primarily target first-order methods and do not directly apply to NTK-DFL. Moreover, these techniques often introduce accuracy degradation in non-IID settings. While momentum acceleration has proven effective in distributed optimization (Polyak, 1964; Nesterov, 1983; Sun et al., 2021), its integration with compressed higher-order methods remains unexplored, as compression-induced noise can destabilize momentum accumulation.

We propose SPARK (Stage-wise Projected NTK and Accelerated Regularization), combining communication-efficient projected NTK, stage-wise annealed knowledge distillation, and Nesterov momentum acceleration. The SPARK framework employs random projections (Johnson & Lindenstrauss, 1984) to aggressively compress Jacobian matrices while preserving spectral properties required for kernel construction. To counteract approximation noise, SPARK integrates a stage-wise annealed distillation strategy that transitions from pure NTK evolution to neighbor-regularized learning, leveraging variance reduction properties of knowledge distillation (Hinton et al., 2015). SPARK incorporates Nesterov momentum (Nesterov, 2004) to dramatically accelerate convergence. The synergistic interplay between distillation and momentum enables stable update accumulation: distillation smooths noisy gradients, allowing momentum to safely accelerate convergence. This co-design achieves the counterintuitive result that aggressive compression paired with intelligent regularization and acceleration yields not only communication efficiency but also faster convergence and superior accuracy compared to the full-rank baseline.

The contributions of this paper are threefold:

1. The proposed SPARK method achieves 98.7% communication reduction compared to NTK-DFL while maintaining convergence speed, and achieves 3 times faster convergence with superior final accuracy when incorporating momentum, establishing new state-of-the-art (SOTA) performance for communication-efficient decentralized federated learning in heterogeneous settings.
2. We establish theoretical convergence guarantees by decomposing optimization error into NTK approximation, projection perturbation, and distillation-based variance reduction terms, formalizing when and why the synergy between compression, distillation, and momentum outperforms static strategies.
3. We validate our approach across multiple network topologies, datasets, and heterogeneity settings to ensure robustness and generalization, demonstrating that SPARK enables practical deployment of NTK-based learning on bandwidth-constrained edge networks.

2. Related Work

Federated and Decentralized Learning Federated learning, introduced by McMahan et al. (2017), enables collaborative model training across distributed clients without sharing raw data, addressing critical privacy and scalability challenges (Zhang et al., 2021; Zhu et al., 2023; Xia et al., 2025). While centralized FL has been improved through methods like SCAFFOLD (Karimireddy et al., 2020) and FedProx (Li et al., 2020) to handle data heterogeneity, the central server architecture introduces communication bottlenecks and single-point privacy risks (Kairouz et al., 2021). Decentralized federated learning (DFL) eliminates the central coordinator by organizing clients in peer-to-peer topologies (Marfoq et al., 2023). Representative DFL approaches include D-PSGD (Lian et al., 2017) for decentralized gradient descent, DFedAvg (Sun et al., 2021) for neighbor averaging, DisPFL (Dai et al., 2022) for personalized sparse training, and DFedSAM (Shi et al., 2023) for sharpness-aware optimization. However, these first-order gradient-based methods exhibit slow convergence under severe statistical heterogeneity, motivating the exploration of higher-order optimization mechanisms and variance reduction techniques.

Neural Tangent Kernel in Federated Learning The neural tangent kernel framework (Jacot et al., 2018) provides a principled theoretical foundation for analyzing infinite-width neural networks through kernel-based linearization (Chizat et al., 2019). Recent work has successfully applied NTK theory to federated settings: Huang et al. (2021) analyzed FedAvg convergence through the NTK lens, Yu et al. (2022) trained convex networks using NTK in centralized FL, and Yue et al. (2022) replaced SGD with NTK-based weight evolution. Most notably, Thompson et al. (2025) extended NTK to decentralized environments, demonstrating significantly faster convergence than existing DFL methods under heterogeneous data distributions. While NTK-DFL achieves superior convergence through expressive kernel-based updates, it faces a critical limitation: transmitting full Jacobian matrices requires substantially higher bandwidth than weight-based methods (Konečný et al., 2016), rendering it impractical for bandwidth-constrained edge environments such as IoT networks operating over LoRaWAN or satellite links. Furthermore, while momentum acceleration has been extensively studied in centralized optimization (Cheng et al., 2024; Yu et al., 2024) and federated settings (Sun et al., 2021), its integration with NTK-based methods remains unexplored, particularly in addressing the instability introduced by aggressive communication compression.

Communication Efficiency and Acceleration Extensive research has addressed communication efficiency through gradient quantization (Alistarh et al., 2017), sparsifica-

tion (Lin et al., 2018), and low-rank factorization (Vogels et al., 2019). However, these first-order compression techniques do not directly apply to NTK’s structured Jacobian matrices and often degrade accuracy under severe compression in non-IID settings. Random projection (Johnson & Lindenstrauss, 1984; Li et al., 2018) and knowledge distillation (Hinton et al., 2015) have been studied separately, but their integration for Jacobian compression remains unexplored. Momentum acceleration (Polyak, 1964; Nesterov, 1983), while effective in decentralized first-order methods (Sun et al., 2021), has not been combined with compressed NTK updates where compression noise introduces stability challenges. In contrast, SPARK synergistically integrates random projection-based Jacobian compression, curriculum-scheduled distillation for variance reduction, and Nesterov momentum for convergence acceleration. By co-designing spatial compression and temporal stabilization, SPARK demonstrates that aggressive compression in NTK-based DFL can simultaneously reduce communication overhead, accelerate convergence, and surpass baseline accuracy—resolving the fundamental tension between communication efficiency and model performance.

3. Proposed Method: SPARK

3.1. Problem Statement

We consider the decentralized federated learning setting where M clients collaboratively train a model without a central server. Each client $i \in \{1, \dots, M\}$ possesses a local dataset $\mathcal{D}_i = \{(\mathbf{x}_i^{(n)}, \mathbf{y}_i^{(n)})\}_{n=1}^{N_i}$, where N_i is the number of local training samples. The clients are connected via an undirected communication graph $\mathcal{G} = (\mathcal{V}, \mathcal{E})$, where \mathcal{V} represents the set of clients and \mathcal{E} denotes the communication edges. Each client i can only communicate with its neighbors $\mathcal{N}_i = \{j \in \mathcal{V} : (i, j) \in \mathcal{E}\}$.

Following the NTK-DFL framework (Thompson et al., 2025), each client maintains a local model \mathbf{w}_i parameterized by weights, and the global objective is to minimize the empirical risk $\mathcal{L}(\mathbf{w}) = \frac{1}{M} \sum_{i=1}^M \mathcal{L}_i(\mathbf{w})$, where

$$\mathcal{L}_i(\mathbf{w}) = \frac{1}{N_i} \sum_{n=1}^{N_i} \ell(f(\mathbf{x}_i^{(n)}; \mathbf{w}), \mathbf{y}_i^{(n)}) \quad (1)$$

is the local empirical loss on client i ’s dataset.

However, NTK-DFL achieves fast convergence by transmitting full Jacobian matrices $\mathbf{J}_i^{(k)} \in \mathbb{R}^{N_i \times C \times d}$ at each round k , where C is the number of output classes and d is the model parameter dimension. For typical edge networks, d can be prohibitively large, creating a communication bottleneck that prevents deployment in bandwidth-constrained environments. Our goal is to retain NTK-DFL’s convergence speed while drastically reducing communication overhead

Algorithm 1 SPARK: Stage-wise Projected NTK and Accelerated Regularization

Require: Graph \mathcal{G} , weights $\{\mathbf{w}_i^{(0)}\}$, proj. dim k , warm-up R_{warm} , total R , momentum μ , hyperparams.
Ensure: Final client models $\{\mathbf{w}_i^{(R)}\}_{i=1}^M$

- 1: Initialize velocity $\mathbf{v}_i^{(0)} \leftarrow \mathbf{0}$ for all clients i
- 2: **for** round $k = 1, \dots, R$ **do**
- 3: **for** client $i \in \{1, \dots, M\}$ **in parallel do**
- 4: $\mathbf{J}_i^{(k)} \leftarrow \text{JACOBIAN}(\mathcal{D}_i; \mathbf{w}_i^{(k)})$; // Compute local Jacobian
- 5: $\tilde{\mathbf{J}}_i^{(k)} \leftarrow \mathbf{J}_i^{(k)} \mathbf{P}_i$; // Compress via random projection
- 6: $\mathbf{z}_i^{(k)} \leftarrow f(\mathbf{X}_i; \mathbf{w}_i^{(k)})$; // Compute local logits
- 7: **send** $\{\tilde{\mathbf{J}}_i^{(k)}, \mathbf{z}_i^{(k)}\}$ **to** \mathcal{N}_i ; // Broadcast to neighbors
- 8: **end for**
- 9: **for** client $i \in \{1, \dots, M\}$ **in parallel do**
- 10: Receive $\{\tilde{\mathbf{J}}_j^{(k)}, \mathbf{z}_j^{(k)}\}_{j \in \mathcal{N}_i}$;
- 11: $\tilde{\mathbf{J}}_{\text{agg}}^{(k)} \leftarrow [\tilde{\mathbf{J}}_i^{(k)}, \{\tilde{\mathbf{J}}_j^{(k)}\}_{j \in \mathcal{N}_i}]$; // Concatenate neighbor Jacobians
- 12: $\mathbf{K}^{(k)} \leftarrow \tilde{\mathbf{J}}_{\text{agg}}^{(k)} (\tilde{\mathbf{J}}_{\text{agg}}^{(k)})^\top$; // Compute empirical NTK
- 13: $\mathbf{Y}_{\text{tgt}}^{(k)} \leftarrow \text{DISTILLTARGET}(k, \dots)$; // See Alg. 2
- 14: $\{\mathbf{f}_t^{(k)}\} \leftarrow \text{KERNELDESCENT}(\mathbf{K}^{(k)}, \mathbf{Y}_{\text{tgt}}^{(k)})$; // Evolve predictions
- 15: $\Delta \mathbf{w}_i^{(k)} \leftarrow \text{BACKPROJ}(\tilde{\mathbf{J}}_{\text{agg}}^{(k)}, \mathbf{Y}_{\text{tgt}}^{(k)}, \{\mathbf{f}_t^{(k)}\})$; // Map to weight space
- 16: $\mathbf{v}_i^{(k+1)} \leftarrow \mu \mathbf{v}_i^{(k)} + \Delta \mathbf{w}_i^{(k)}$; // Update velocity
- 17: $\mathbf{w}_i^{(k+1)} \leftarrow \mathbf{w}_i^{(k)} + \mu \mathbf{v}_i^{(k+1)} + \Delta \mathbf{w}_i^{(k)}$; // Nesterov update
- 18: **end for**
- 19: **end for**

through aggressive compression paired with intelligent stabilization mechanisms.

3.2. Proposed SPARK Framework

We present SPARK, a Stage-wise Projected NTK and Accelerated Regularization method that resolves the communication-convergence trade-off in NTK-DFL through a principled co-design of spatial compression, temporal stabilization, and convergence acceleration. The framework integrates three key components: random projection for Jacobian compression, stage-wise annealed distillation for training stabilization, and Nesterov momentum for convergence acceleration. Figure 1 illustrates the overall framework.

Spatial compression via random projection. The core innovation of SPARK is the use of random projections to compress Jacobian matrices while preserving their spectral properties. For each layer ℓ with parameter dimension d_ℓ ,

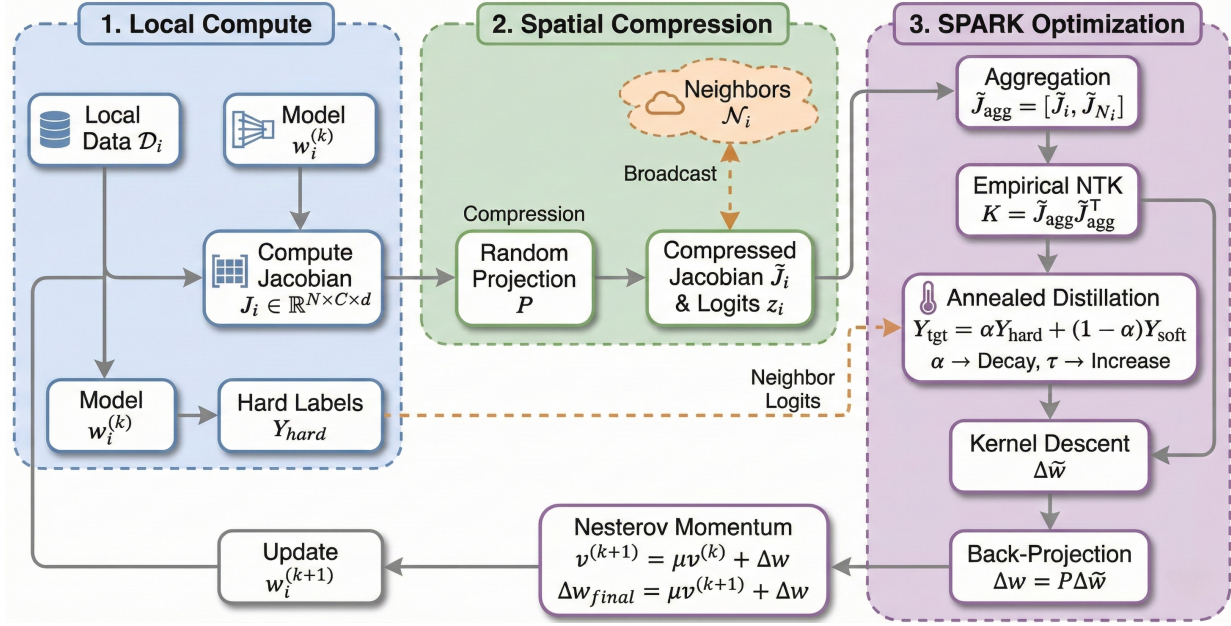


Figure 1. Overview of the SPARK framework integrating spatial compression via random projection, temporal stabilization via annealed distillation, and convergence acceleration via Nesterov momentum. Clients compute compressed Jacobians, exchange logits for distillation, and evolve models through kernel regression with momentum.

Algorithm 2 Stage-wise Annealed Distillation Target Construction

Require: Round k , thresholds R_{warm}, R , labels \mathbf{Y}_{hard} , logits $\{\mathbf{z}_j\}$, hyperparams.

Ensure: Distillation target $\mathbf{Y}_{\text{target}}$

- 1: **if** $k \leq R_{\text{warm}}$ **then**
- 2: $\alpha \leftarrow 1.0, \tau \leftarrow 1.0$; // Initialize: Pure NTK phase
- 3: **else**
- 4: $p \leftarrow (k - R_{\text{warm}}) / (R - R_{\text{warm}})$; // Calculate progress ratio
- 5: $\alpha \leftarrow \alpha_{\text{final}} + \frac{1}{2}(\alpha_{\text{init}} - \alpha_{\text{final}})(1 + \cos(\pi p))$; // Update mixing coef.
- 6: $\tau \leftarrow \tau_{\text{init}} + (\tau_{\text{final}} - \tau_{\text{init}})p$; // Update temperature
- 7: **end if**
- 8: Aggregate neighbor logits: $\mathbf{z}_{\text{agg}} = [\mathbf{z}_i; \mathbf{z}_{j_1}; \dots; \mathbf{z}_{j_{|\mathcal{N}_i|}}]$
- 9: Compute soft labels: $\mathbf{Y}_{\text{soft}} = \text{softmax}(\mathbf{z}_{\text{agg}} / \tau)$
- 10: Construct target: $\mathbf{Y}_{\text{target}} = \alpha \mathbf{Y}_{\text{hard}} + (1 - \alpha) \mathbf{Y}_{\text{soft}}$
- 11: **return** $\mathbf{Y}_{\text{target}}$

we generate a deterministic random projection matrix $\mathbf{P}_\ell \in \mathbb{R}^{d_\ell \times k}$ using a layer-specific seed derived from a global random seed. The projection matrix is sampled as:

$$\mathbf{P}_\ell \sim \mathcal{N}(0, k^{-1} \mathbf{I}), \quad \text{with entries } P_{\ell,ij} \sim \mathcal{N}(0, 1/k), \quad (2)$$

where the scaling factor $k^{-1/2}$ ensures that the projection approximately preserves inner products with high probability. This design is grounded in the Johnson-Lindenstrauss

lemma (Johnson & Lindenstrauss, 1984), which guarantees that for any two vectors $\mathbf{u}, \mathbf{v} \in \mathbb{R}^{d_\ell}$, the distance preservation property holds when the projection dimension satisfies $k = \Omega(\epsilon^{-2} \log d_\ell)$ for a desired distortion $\epsilon > 0$.

For a client i with Jacobian $\mathbf{J}_i^{(k)} = [\mathbf{J}_{i,\ell}^{(k)}]_\ell \in \mathbb{R}^{N_i \times C \times d}$, where $\mathbf{J}_{i,\ell}^{(k)} \in \mathbb{R}^{N_i \times C \times d_\ell}$ is the Jacobian for layer ℓ , the compressed Jacobian is computed as:

$$\tilde{\mathbf{J}}_{i,\ell}^{(k)} = \mathbf{J}_{i,\ell}^{(k)} \mathbf{P}_\ell \in \mathbb{R}^{N_i \times C \times k}. \quad (3)$$

The total communication volume is reduced from $\text{sizeof}(\mathbf{J}_i^{(k)}) = N_i \cdot C \cdot d$ to $\text{sizeof}(\tilde{\mathbf{J}}_i^{(k)}) = N_i \cdot C \cdot k$, achieving a compression ratio:

$$\rho = \frac{k}{d} \ll 1, \quad (4)$$

which enables substantial bandwidth savings. A critical design choice is that projection matrices \mathbf{P}_ℓ are deterministically generated using layer-specific seeds $s_\ell = \text{Hash}(s_{\text{global}} \parallel \text{name}_\ell)$, where \parallel denotes concatenation and Hash is a cryptographic hash function. This ensures that all clients use identical projection matrices for the same layer, enabling correct kernel computation, and that the projection is consistent across all communication rounds, preventing approximation drift. Importantly, no additional communication is needed to synchronize projection matrices.

After receiving compressed Jacobians $\{\tilde{\mathbf{J}}_j^{(k)}\}_{j \in \mathcal{N}_i \cup \{i\}}$ from neighbors, client i constructs an aggregated Jacobian by

concatenating along the sample dimension:

$$\tilde{\mathbf{J}}_{\text{agg}}^{(k)} = [\tilde{\mathbf{J}}_i^{(k)}; \tilde{\mathbf{J}}_{j_1}^{(k)}; \dots; \tilde{\mathbf{J}}_{j_{|\mathcal{N}_i|}}^{(k)}] \in \mathbb{R}^{N_{\text{agg}} \times C \times k}, \quad (5)$$

where $N_{\text{agg}} = \sum_{j \in \mathcal{N}_i \cup \{i\}} N_j$ is the total number of samples from the client and its neighbors. The empirical Neural Tangent Kernel is then computed as:

$$\mathbf{K}^{(k)} = \tilde{\mathbf{J}}_{\text{agg}}^{(k)} (\tilde{\mathbf{J}}_{\text{agg}}^{(k)})^\top \in \mathbb{R}^{(N_{\text{agg}} \cdot C) \times (N_{\text{agg}} \cdot C)}. \quad (6)$$

This kernel matrix encodes the geometry of the loss landscape in the compressed parameter space, where each entry $K_{ij}^{(k)} = \langle \tilde{\mathbf{J}}_{\text{agg},i}^{(k)}, \tilde{\mathbf{J}}_{\text{agg},j}^{(k)} \rangle$ measures the similarity between training sample pairs. Although $\tilde{\mathbf{J}}_{\text{agg}}^{(k)}$ is an approximation of the full Jacobian, the kernel $\mathbf{K}^{(k)}$ provably captures the essential spectral structure needed for convergence.

Temporal stabilization via stage-wise annealed distillation. To counteract the approximation noise introduced by aggressive compression, SPARK integrates a novel knowledge distillation strategy that leverages neighbor predictions as soft regularization targets. The key insight is that soft labels from neighboring clients provide complementary information that can compensate for compression-induced errors while maintaining training stability.

The distillation strategy operates in two distinct phases. During the initial warmup period spanning rounds $k \in \{1, \dots, R_{\text{warm}}\}$, we use only ground-truth hard labels as training targets with mixing coefficient $\alpha^{(k)} = 1.0$ and temperature parameter $\tau^{(k)} = 1.0$. This allows the projected NTK to establish a good initialization without interference from potentially noisy soft targets. After the warmup phase, we gradually transition to a mixture of hard and soft labels. The mixing coefficient $\alpha^{(k)}$ follows a cosine annealing schedule, while the temperature parameter $\tau^{(k)}$ increases linearly to progressively soften the probability distributions.

Specifically, for a given round $k > R_{\text{warm}}$, we compute the progress ratio:

$$p^{(k)} = \frac{k - R_{\text{warm}}}{R - R_{\text{warm}}} \in [0, 1], \quad (7)$$

where R_{warm} is the number of warmup rounds and R is the total number of rounds. The mixing coefficient and temperature are then updated as:

$$\alpha^{(k)} = \alpha_{\text{final}} + \frac{1}{2}(\alpha_{\text{init}} - \alpha_{\text{final}})(1 + \cos(\pi p^{(k)})), \quad (8)$$

$$\tau^{(k)} = \tau_{\text{init}} + (\tau_{\text{final}} - \tau_{\text{init}})p^{(k)}. \quad (9)$$

The soft labels are constructed by aggregating logits $\mathbf{z}_j^{(k)} \in \mathbb{R}^{N_j \times C}$ from all neighbors and the client itself to form $\mathbf{z}_{\text{agg}}^{(k)} \in \mathbb{R}^{N_{\text{agg}} \times C}$, then applying temperature-scaled softmax:

$$\mathbf{Y}_{\text{soft},nc}^{(k)} = \frac{\exp(z_{\text{agg},nc}^{(k)} / \tau^{(k)})}{\sum_{c'=1}^C \exp(z_{\text{agg},nc'}^{(k)} / \tau^{(k)})}. \quad (10)$$

The final target for kernel evolution is:

$$\mathbf{Y}_{\text{target}}^{(k)} = \alpha^{(k)} \mathbf{Y}_{\text{hard}} + (1 - \alpha^{(k)}) \mathbf{Y}_{\text{soft}}^{(k)}, \quad (11)$$

where $\mathbf{Y}_{\text{hard}} \in \{0, 1\}^{N_{\text{agg}} \times C}$ denotes the one-hot encoded ground-truth labels. This curriculum-based approach acts as a variance reduction mechanism, smoothing the noisy gradients induced by projection, while enabling implicit knowledge sharing across the graph topology.

Convergence acceleration via momentum optimization.

Beyond compression and stabilization, SPARK incorporates momentum-based optimization to dramatically accelerate convergence. Traditional NTK-based methods evolve predictions through direct kernel-based updates, which can converge slowly under high data heterogeneity. SPARK addresses this by maintaining a velocity term that accumulates gradient information across rounds.

Specifically, let $\mathbf{w}_i^{(k)}$ denote client i 's model weights at round k , and let $\Delta \mathbf{w}_i^{(k)}$ be the weight update computed from kernel-based prediction evolution (detailed below). We maintain a velocity vector $\mathbf{v}_i^{(k)} \in \mathbb{R}^d$ that is updated as:

$$\mathbf{v}_i^{(k+1)} = \mu \mathbf{v}_i^{(k)} + \Delta \mathbf{w}_i^{(k)}, \quad (12)$$

where $\mu \in [0, 1]$ is the momentum coefficient. The momentum term $\mu \mathbf{v}_i^{(k)}$ accumulates historical gradient information, enabling the optimization to maintain direction through noisy updates and accelerate convergence along consistent descent directions.

SPARK employs Nesterov accelerated momentum (Nesterov, 2004), which provides superior convergence guarantees compared to standard momentum. The Nesterov update applies a lookahead step:

$$\mathbf{w}_i^{(k+1)} = \mathbf{w}_i^{(k)} + \mu \mathbf{v}_i^{(k+1)} + \Delta \mathbf{w}_i^{(k)}. \quad (13)$$

This lookahead mechanism enables more informed update decisions. We set $\mu = 0.9$, providing strong momentum effects while maintaining stability. The momentum mechanism is particularly effective in the NTK regime, where kernel-based evolution ensures stable update directions that can be safely accumulated. Critically, stage-wise annealed distillation further stabilizes momentum-driven training by smoothing noisy gradients.

Kernel-based prediction evolution and weight updates.

Given the empirical kernel $\mathbf{K}^{(k)}$ and target labels $\mathbf{Y}_{\text{target}}^{(k)}$, we evolve the network predictions via kernel-based gradient descent. Starting from the current model's predictions $\mathbf{f}_0^{(k)} = f(\mathbf{X}_{\text{agg}}; \mathbf{w}_i^{(k)})$, the prediction trajectory is computed as:

$$\mathbf{f}_t^{(k)} = \mathbf{f}_0^{(k)} - \eta \sum_{s=0}^{t-1} \mathbf{K}^{(k)} \nabla_{\mathbf{f}} \mathcal{L}(\mathbf{f}_s^{(k)}, \mathbf{Y}_{\text{target}}^{(k)}), \quad (14)$$

where η is the learning rate and $\nabla_{\mathbf{f}} \mathcal{L}$ is the gradient with respect to predictions. For cross-entropy loss, this reduces to:

$$\mathbf{f}_t^{(k)} = \mathbf{f}_0^{(k)} + \eta \mathbf{K}^{(k)} \left(\mathbf{Y}_{\text{target}}^{(k)} - \sum_{s=0}^{t-1} \text{softmax}(\mathbf{f}_s^{(k)}) \right). \quad (15)$$

We evolve predictions for multiple timesteps and select the timestep $t^* = \arg \min_t \mathcal{L}_{\text{val}}(\mathbf{f}_t^{(k)})$ that minimizes validation loss. After obtaining the optimal prediction trajectory, we compute weight updates in the compressed space:

$$\Delta \tilde{\mathbf{w}}_{t^*} = -\frac{\eta}{N_{\text{agg}}} (\tilde{\mathbf{J}}_{\text{agg}}^{(k)})^\top \left(\sum_{s=0}^{t^*-1} \text{softmax}(\mathbf{f}_s^{(k)}) - t^* \mathbf{Y}_{\text{target}}^{(k)} \right), \quad (16)$$

where $\Delta \tilde{\mathbf{w}}_{t^*} \in \mathbb{R}^k$ represents the gradient in the compressed subspace. To obtain the update in the original parameter space, we apply the back-projection:

$$\Delta \mathbf{w}_{t^*} = \mathbf{P} \Delta \tilde{\mathbf{w}}_{t^*} \in \mathbb{R}^d. \quad (17)$$

This back-projection step ensures the update is compatible with the original model parameters. The final model update incorporates momentum as described in Equations 12 and 13.

Communication and computational efficiency. We now analyze the overhead of SPARK compared to NTK-DFL. For a network with M clients, average degree $|\mathcal{N}|$, batch size N , C classes, and parameter dimension d , NTK-DFL requires $O(M \cdot |\mathcal{N}| \cdot N \cdot C \cdot d)$ total communication per round, while SPARK requires $O(M \cdot |\mathcal{N}| \cdot N \cdot C \cdot k)$ per round, achieving a compression ratio of $\rho = k/d$. The computational overhead of SPARK is minimal: the projection operation $\tilde{\mathbf{J}}_i^{(k)} = \mathbf{J}_i^{(k)} \mathbf{P}$ costs $O(N \cdot C \cdot d \cdot k)$ operations, comparable to the Jacobian computation itself. The dominant cost remains the empirical kernel computation with complexity $O((N_{\text{agg}} \cdot C)^2 \cdot k)$, which is faster than NTK-DFL's $O((N_{\text{agg}} \cdot C)^2 \cdot d)$ by a factor of d/k . The momentum update adds negligible overhead of $O(d)$ per round. Thus, SPARK achieves both communication and computational efficiency gains while dramatically accelerating convergence through momentum.

4. Theoretical Analysis

We provide a lightweight non-convex convergence guarantee for SPARK. The bound decomposes into an approximation bias term induced by projected-NTK back-projection and a variance term controlled by the stage-wise annealed distillation schedule.

Global objective. Let $\mathcal{L}(w) = \frac{1}{M} \sum_{i=1}^M \mathcal{L}_i(w)$ be the global objective. At round t , each client computes a back-projected update $\Delta w_i^{(t)}$ and performs the (Nesterov-style)

momentum step

$$\begin{aligned} v_i^{(t+1)} &= \mu v_i^{(t)} + \Delta w_i^{(t)}, \\ w_i^{(t+1)} &= w_i^{(t)} + \mu v_i^{(t+1)} + \Delta w_i^{(t)}. \end{aligned} \quad (18)$$

where $\mu \in [0, 1]$. Define averages $\bar{w}^{(t)} = \frac{1}{M} \sum_{i=1}^M w_i^{(t)}$, $\bar{v}^{(t)} = \frac{1}{M} \sum_{i=1}^M v_i^{(t)}$, and $\bar{\Delta}^{(t)} = \frac{1}{M} \sum_{i=1}^M \Delta w_i^{(t)}$.

Definition 4.1. (Projected NTK subspace). Let $P \in \mathbb{R}^{d \times k}$ ($k < d$) be a fixed random projection matrix shared by all clients and assume P has full column rank. Define the orthogonal projector onto $\text{Range}(P)$ as

$$\Pi \triangleq P(P^\top P)^{-1} P^\top. \quad (19)$$

SPARK's back-projected NTK update operates in $\text{Range}(\Pi)$, and the ideal projected descent direction at w is $\Pi \nabla \mathcal{L}_i(w)$.

Definition 4.2. (Annealed distillation objective). At round t , SPARK forms the distillation target

$$Y_{\text{tgt}}^{(t)} = \alpha^{(t)} Y_{\text{hard}} + (1 - \alpha^{(t)}) Y_{\text{soft}}^{(t)}, \quad (20)$$

where $\alpha^{(t)} \in [0, 1]$ and $\tau^{(t)} \geq 1$ follow the stage-wise schedule. Let $p_{\tau^{(t)}}(w) \triangleq \text{softmax}(f(x; w)/\tau^{(t)})$. Define the effective local objective

$$\begin{aligned} \mathcal{L}_i^{(t)}(w) &\triangleq \alpha^{(t)} \mathcal{L}_i^{\text{CE}}(w) + (1 - \alpha^{(t)}) \tau^{(t)2} \\ &\quad \cdot \text{KL}(Y_{\text{soft}}^{(t)} \| p_{\tau^{(t)}}(w)). \end{aligned} \quad (21)$$

The update $\Delta w_i^{(t)}$ is computed via projected-NTK evolution using $(Y_{\text{tgt}}^{(t)}, P)$ and then back-projected to \mathbb{R}^d .

Assumption 4.3. (Smoothness and annealed stochasticity). For all clients i and rounds t , we assume \mathcal{L} and each $\mathcal{L}_i^{(t)}$ are L -smooth. Moreover, there exist $\sigma^2 > 0$ and a non-increasing sequence $\{\gamma_t\}_{t \geq 0} \subset (0, 1]$ such that, with filtration \mathcal{F}_t ,

$$\mathbb{E} \left[\left\| \Delta w_i^{(t)} - \mathbb{E}[\Delta w_i^{(t)} | \mathcal{F}_t] \right\|^2 \middle| \mathcal{F}_t \right] \leq \eta^2 \sigma^2 \gamma_t. \quad (22)$$

Conditioned on \mathcal{F}_t , the client update noises are uncorrelated across clients.

Assumption 4.4. (Projected-NTK approximation bias). Let $\bar{\Delta}_{\mathbb{E}}^{(t)} \triangleq \mathbb{E}[\bar{\Delta}^{(t)} | \mathcal{F}_t]$. Define the momentum virtual sequence

$$\bar{z}^{(t)} \triangleq \bar{w}^{(t)} + \frac{\mu^2}{1 - \mu} \bar{v}^{(t)}. \quad (23)$$

We assume there exists $\delta_{\text{total}} \geq 0$ such that for all t ,

$$\left\| \bar{\Delta}_{\mathbb{E}}^{(t)} + \eta \nabla \mathcal{L}(\bar{z}^{(t)}) \right\| \leq \eta \delta_{\text{total}}. \quad (24)$$

We interpret δ_{total} as the aggregate bias caused by projection, finite-width NTK approximation, and decentralized neighbor-aggregation mismatch (graph-induced discrepancy).

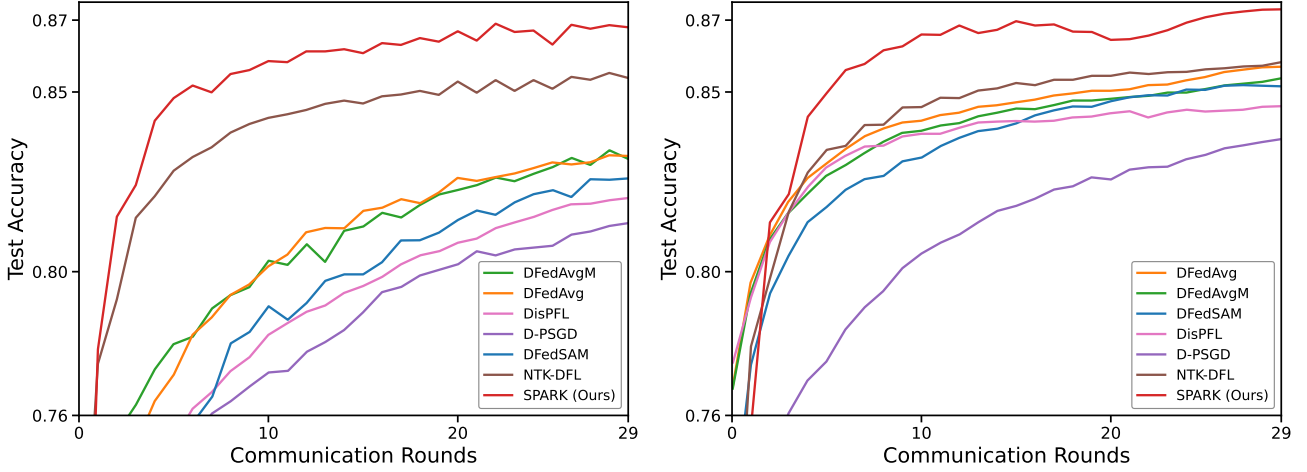


Figure 2. Convergence of different methods on Fashion-MNIST for highly non-IID with $\alpha = 0.1$ and IID settings. SPARK maintains NTK-DFL’s convergence speed while achieving substantial communication reduction.

Theorem 4.5. (Convergence of SPARK (non-convex)). Under Assumptions 4.3–4.4, assume the stepsize satisfies

$$\eta \leq \frac{1 - \mu}{4L}. \quad (25)$$

Let $\bar{\gamma} \triangleq \frac{1}{T} \sum_{t=0}^{T-1} \gamma_t$. Then after T rounds,

$$\begin{aligned} \min_{0 \leq t < T} \mathbb{E} \|\nabla \mathcal{L}(\bar{z}^{(t)})\|^2 &\leq \frac{2(1 - \mu)(\mathcal{L}(\bar{z}^{(0)}) - \mathcal{L}^*)}{\eta T} \\ &\quad + \frac{C_1 L \eta \sigma^2}{M(1 - \mu)} \bar{\gamma} + C_2 \delta_{\text{total}}^2, \end{aligned} \quad (26)$$

where C_1, C_2 are absolute constants independent of T .

Corollary 4.6. (Communication–accuracy trade-off). Choosing $\eta = \Theta(1/\sqrt{T})$ yields

$$\min_{0 \leq t < T} \mathbb{E} \|\nabla \mathcal{L}(\bar{z}^{(t)})\|^2 = \mathcal{O}\left(\frac{1}{\sqrt{T}} + \frac{\bar{\gamma}}{M\sqrt{T}} + \delta_{\text{total}}^2\right). \quad (27)$$

Per round, SPARK communicates objects of dimension k instead of d ; hence the compression ratio is $\rho = k/d$ and the reduction factor scales as d/k .

From (27), the convergence rate naturally decomposes into an optimization term, a stochastic term, and an approximation-bias floor. Specifically, increasing T reduces the optimization error as $\mathcal{O}(1/\sqrt{T})$, while the stochastic contribution is further suppressed by both client averaging (scaling as $1/M$) and the stage-wise annealed distillation schedule through the factor $\bar{\gamma}$. In contrast, δ_{total}^2 captures the aggregate bias induced by projected-NTK back-projection and decentralized mismatch, which forms an irreducible error floor and cannot be eliminated solely by running more rounds. Therefore, SPARK achieves communication savings by exchanging k -dimensional objects per round while

preserving convergence up to the bias floor determined by δ_{total} .

5. Experiments

5.1. Experimental Setup

Datasets and Model Following Thompson et al. (2025), we evaluate on Fashion-MNIST (Xiao et al., 2017) with 60,000 training and 10,000 test samples across 10 categories. Data heterogeneity is introduced via symmetric Dirichlet distribution with concentration parameter α (Hsu et al., 2019), where smaller α creates higher label skewness. For each client i , we sample $\mathbf{q}_i \sim \text{Dir}(\alpha \mathbf{1})$ with $\mathbf{q}_i \in \mathbb{R}^{10}$ defining label probabilities. We test across multiple α values to evaluate robustness. The model is a two-layer MLP with 100 hidden neurons, yielding $d = 79,510$ parameters.

Network Topology We employ a sparse, time-variant κ -regular graph with $\kappa = 5$ across $M = 300$ clients. At each communication round, a new random graph with the same degree is generated. This sparse connectivity reflects realistic decentralized settings with limited peer connections while ensuring fairness across all methods.

Baselines We compare SPARK against state-of-the-art decentralized methods including D-PSGD (Lian et al., 2017), D-FedAvg, D-FedAvgM (Sun et al., 2021), D-FedSAM (Shi et al., 2023), and DisPFL (Dai et al., 2022), as well as the baseline NTK-DFL (Thompson et al., 2025).

Evaluation Metrics We measure test accuracy on a global holdout set to evaluate model generalization from heterogeneous local data. This aligns with the objective of training a global model with improved generalization, consistent with standard federated learning evaluation (Tan et al., 2022).

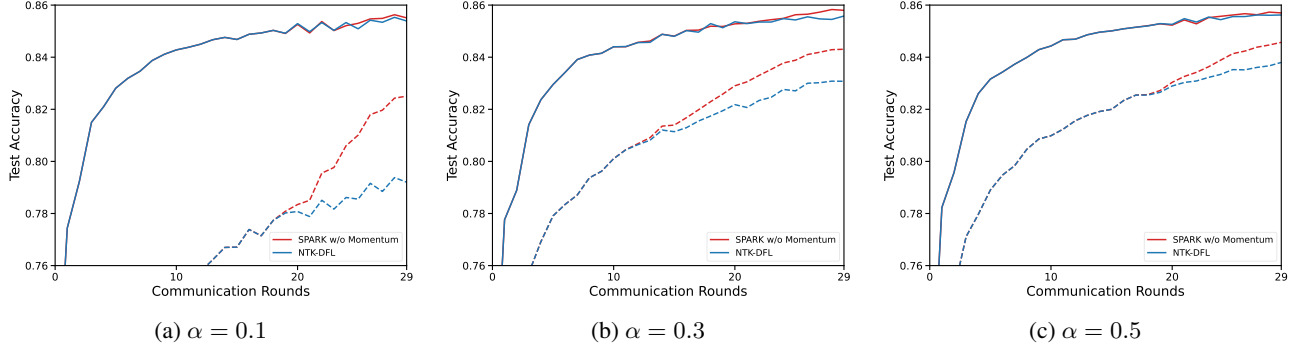


Figure 3. Convergence performance under different Non-IID settings with $\alpha \in \{0.1, 0.3, 0.5\}$. Solid lines show aggregated model accuracy; dashed lines show average client accuracy. SPARK without momentum significantly outperforms NTK-DFL in average client accuracy, validating that distillation effectively bridges the performance gap between local and global models.

Table 1. Communication rounds to reach 85% test accuracy on Fashion-MNIST. SPARK with momentum achieves significant convergence acceleration across all heterogeneity levels.

Method	IID	$\alpha = 0.5$	$\alpha = 0.1$
DFedAvg	18	31	83
DFedAvgM	23	43	86
DFedSAM	24	45	200+
DisPFL	43	87	200+
D-PSGD	53	79	125
NTK-DFL	13	15	18
SPARK (w/o Momentum)	13	14	18
SPARK	6	6	6

Table 2. Effect of Projection Dimension on Convergence and Efficiency.

Method	Proj. Dim. (k)	Comm. Red. (%)	Rounds to 85%	Final Acc. (%)
NTK-DFL	79,510	0.0	18	85.38
	500	99.4	27	85.02
SPARK (w/o Momentum)	750	99.1	18	85.39
	1,000	98.7	18	85.51
SPARK	1,000	98.7	6	86.80

5.2. Experimental Results

Test Accuracy & Convergence Figure 2 illustrates convergence trajectories across heterogeneity settings on Fashion-MNIST. Under high heterogeneity with $\alpha = 0.1$, SPARK without momentum maintains NTK-DFL’s convergence speed, reaching 85% accuracy in 18 rounds while achieving 98.7% communication reduction with projection dimension $k = 1,000$. Complete SPARK with momentum dramatically accelerates convergence to just 6 rounds across all heterogeneity levels, as shown in Table 1. For the highly heterogeneous setting with $\alpha = 0.1$, this represents 3 times faster convergence compared to the baseline and 13.8 times improvement over DFedAvg, the next best performing

Table 3. Test accuracy comparison under varying data heterogeneity levels. Smaller α indicates higher heterogeneity.

Method	Heterogeneity Level (α)		
	$\alpha = 0.1$	$\alpha = 0.3$	$\alpha = 0.5$
D-PSGD (Lian et al., 2017)	81.05	82.54	82.61
DFedSAM (Shi et al., 2023)	82.60	83.70	84.63
DisPFL (Dai et al., 2022)	83.09	84.13	83.97
DFedAvgM (Sun et al., 2021)	83.21	84.43	84.71
DFedAvg (Sun et al., 2021)	83.51	84.66	84.78
NTK-DFL (Thompson et al., 2025)	85.53	85.58	85.62
SPARK (w/o Momentum)	85.63	85.83	85.73
SPARK	86.90	86.71	86.66

traditional baseline.

Factor Analyses for SPARK We evaluate SPARK’s performance across projection dimensions and heterogeneity levels. Table 2 demonstrates the impact of projection dimension on communication efficiency. With $k = 1,000$, SPARK without momentum achieves 98.7% communication reduction while maintaining 18-round convergence and surpassing baseline accuracy. This represents optimal compression: higher dimensions like $k = 5,000$ offer no accuracy improvement while requiring 5 times more communication, whereas lower dimensions like $k = 500$ require additional rounds to converge. Complete SPARK with momentum further accelerates convergence to 6 rounds while achieving 86.80% final accuracy, demonstrating the synergistic benefits of projection and momentum.

Table 3 presents performance across varying heterogeneity levels. SPARK consistently outperforms both state-of-the-art decentralized baselines and NTK-DFL across all settings. Notably, SPARK without momentum already improves upon NTK-DFL through distillation, while complete SPARK with momentum achieves substantial additional gains. Under the most challenging setting with $\alpha = 0.1$, SPARK achieves

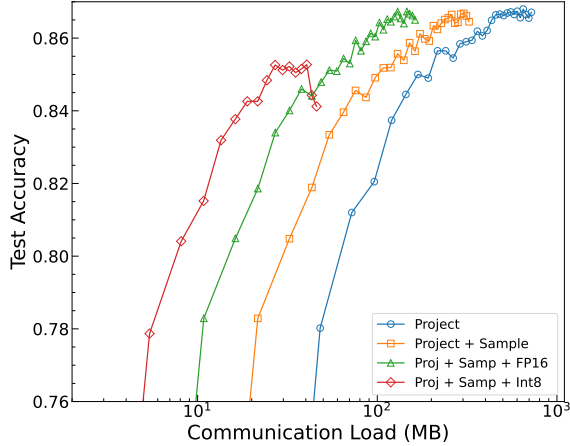


Figure 4. Communication-accuracy trade-offs for progressive compression optimizations on Fashion-MNIST ($\alpha = 0.1$). Combining projection, sampling, and FP16 quantization achieves optimal compression with stable training.

86.90% accuracy, representing 1.37 percentage point improvement over the baseline. The consistent improvements across all heterogeneity levels demonstrate SPARK’s robust resilience to non-IID data distributions.

Figure 3 provides deeper insights by comparing aggregated model accuracy with average client model accuracy under different heterogeneity settings. While NTK-DFL achieves high global accuracy through post-training aggregation, it exhibits a significant generalization gap between global consensus and individual local models. SPARK addresses this through stage-wise annealed distillation. Under the most heterogeneous setting with $\alpha = 0.1$, SPARK improves average client accuracy from 75% to 82.5%, narrowing the generalization gap by 7.5 percentage points while maintaining aggregated performance at 86.9%. This demonstrates that distillation creates beneficial inter-client model diversity during training, which enhances both individual client performance and global model generalization when exploited through model averaging. Similar improvements are observed across all heterogeneity levels, with the performance gap decreasing as data becomes less heterogeneous.

Communication Efficiency Figure 4 demonstrates progressive compression optimizations. Random projection provides substantial communication reduction, while data sampling and quantization offer compounding benefits. With projection dimension $k = 530$ and 45% sampling, FP16 quantization achieves 77.5% reduction from projection alone while maintaining stable convergence to 86.5% accuracy, representing the optimal balance between compression efficiency and training stability. Although Int8 quantization provides higher compression, it suffers from training instability in later rounds, with accuracy declining after round 17. FP16 thus emerges as the preferred

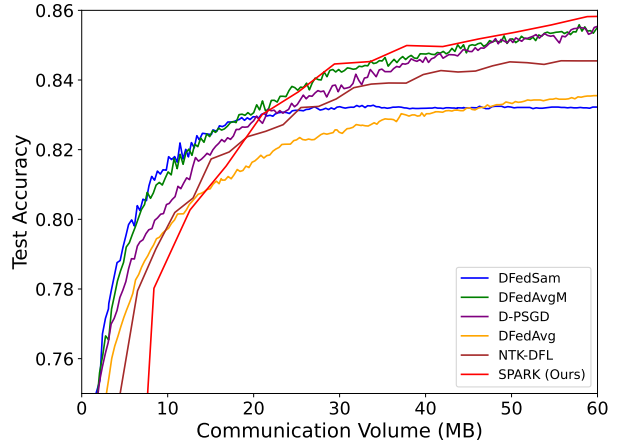


Figure 5. Test accuracy vs. communication volume on Fashion-MNIST ($\alpha = 0.1$). SPARK converges faster to 85% accuracy and achieves higher final performance compared to NTK-DFL and other decentralized baselines.

Table 4. Ablation study on SPARK components under non-IID and IID settings.

Method	Non-IID ($\alpha = 0.1$)			IID		
	Rounds to 85%	Agg. Acc. (%)	Client Acc. (%)	Rounds to 85%	Agg. Acc. (%)	Client Acc. (%)
Baseline (NTK-DFL)	18	85.53	79.38	13	85.83	85.24
Variant A (Proj. only)	18	85.53	79.38	13	85.83	85.24
Variant B (Proj. + Dist.)	18	85.63	82.43	13	86.02	85.51
Variant C (Proj. + Mom.)	6	86.90	82.98	6	86.97	85.49
SPARK (Ours)	6	86.90	82.98	6	87.30	86.53

quantization strategy for production deployments.

Figure 5 compares SPARK against decentralized baseline methods across varying communication budgets. SPARK demonstrates competitive performance with other methods in early training stages and achieves superior final accuracy compared to DFedAvgM, DFedAvg, DFedSam, and D-PSGD. Compared to compressed NTK-DFL, SPARK converges faster to 85% accuracy and achieves higher final performance, demonstrating superior communication-accuracy trade-offs. These results validate that random projection with sampling and quantization effectively preserves NTK dynamics while achieving practical communication efficiency.

Ablation Study To validate the contribution of each component, we decompose SPARK into random projection for communication efficiency, stage-wise annealed distillation for collaborative learning, and momentum optimization for convergence acceleration. Table 4 and Figure 6 present ablation results: Variant A uses projection only, Variant B combines projection with distillation, Variant C combines projection with momentum, and complete SPARK integrates all components.

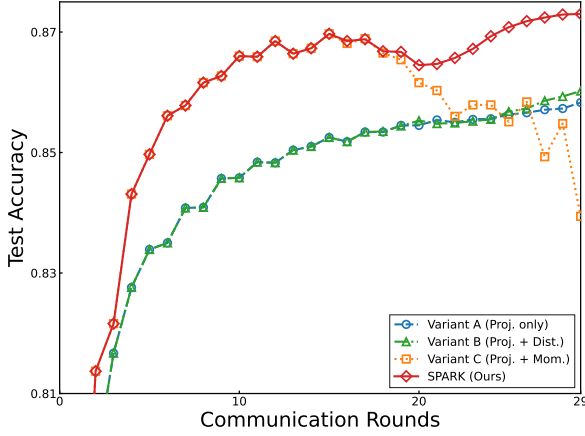


Figure 6. Convergence comparison of ablation variants under IID setting on Fashion-MNIST.

Variant A preserves accuracy identical to NTK-DFL while achieving 98.7% communication reduction. Variant B demonstrates distillation improves both client generalization and aggregated accuracy. Variant C achieves dramatic convergence acceleration and significantly higher aggregated accuracy, demonstrating momentum’s substantial impact. However, as shown in Figure 6, Variant C exhibits severe instability after round 15, with accuracy declining sharply.

Complete SPARK addresses this by integrating distillation with momentum. Distillation stabilizes momentum-driven training, enabling SPARK to maintain rapid convergence while achieving even higher aggregated accuracy. As demonstrated in Table 4, SPARK achieves optimal performance across both settings, validating that distillation is essential for stabilizing momentum and enabling superior final performance.

6. Conclusion

In this paper, we have introduced SPARK, a communication-efficient approach to decentralized federated learning that synergistically integrates random projection-based Jacobian compression, stage-wise annealed knowledge distillation, and Nesterov momentum acceleration. Our work demonstrates that aggressive compression paired with intelligent regularization can simultaneously achieve substantial communication reduction, accelerated convergence, and superior accuracy compared to existing approaches. Extensive experiments validate that SPARK maintains robust performance across diverse network topologies and heterogeneity levels, establishing state-of-the-art results for communication-efficient decentralized federated learning. Future directions include extending SPARK to modern architectures such as convolutional and transformer networks, investigating adaptive projection strategies, and exploring applications in cross-silo federated learning scenarios.

References

- Alistarh, D., Grubic, D., Li, J., Tomioka, R., and Vojnovic, M. Qsgd: Communication-efficient sgd via gradient quantization and encoding. In *Advances in Neural Information Processing Systems*, volume 30, 2017.
- Cheng, Z., Huang, X., Wu, P., and Yuan, K. Momentum benefits non-IID federated learning simply and provably. In *The Twelfth International Conference on Learning Representations*, 2024. URL <https://openreview.net/forum?id=TdhkAcXkRi>.
- Chizat, L., Oyallon, E., and Bach, F. On lazy training in differentiable programming. *Advances in Neural Information Processing Systems*, 32, 2019.
- Dai, Y., Wang, Z., Li, Y., Verbraeken, J., and Pan, S. Displf: Towards communication-efficient personalized federated learning via decentralized sparse training. In *International Conference on Machine Learning*, pp. 4587–4604. PMLR, 2022.
- Hinton, G., Vinyals, O., and Dean, J. Distilling the knowledge in a neural network. *arXiv preprint arXiv:1503.02531*, 2015.
- Hsu, T.-M. H., Qi, H., and Brown, M. Measuring the effects of non-identical data distribution for federated visual classification. In *NeurIPS Workshop on Federated Learning for Data Privacy and Confidentiality*, 2019.
- Huang, S. P. K., Reddi, S. J., Kale, S., and Suresh, A. T. An analysis of federated learning in the ntk regime. In *NeurIPS 2021 Workshop on New Frontiers in Federated Learning*, 2021.
- Jacot, A., Gabriel, F., and Hongler, C. Neural tangent kernel: Convergence and generalization in neural networks. In *Advances in neural information processing systems*, volume 31, 2018.
- Johnson, W. B. and Lindenstrauss, J. Extensions of lipschitz mappings into a hilbert space. *Contemporary mathematics*, 26(189-206):1, 1984.
- Kairouz, P., McMahan, H. B., Avent, B., Bellet, A., Bennis, M., Bhagoji, A. N., Bonawitz, K., Charles, Z., Cormode, G., Cummings, R., et al. Advances and open problems in federated learning. *Foundations and Trends in Machine Learning*, 14(1–2):1–210, 2021.
- Karimireddy, S. P., Kale, S., Mohri, M., Reddi, S., Stich, S., and Suresh, A. T. Scaffold: Stochastic controlled averaging for federated learning. In *International Conference on Machine Learning*, pp. 5132–5143. PMLR, 2020.

- Konečný, J., McMahan, H. B., Yu, F. X., Richtárik, P., Suresh, A. T., and Bacon, D. Federated learning: Strategies for improving communication efficiency. *arXiv preprint arXiv:1610.05492*, 2016.
- Li, C., Farkhoor, H., Liu, R., and Yosinski, J. Measuring the intrinsic dimension of objective landscapes. In *International Conference on Learning Representations*, 2018.
- Li, T., Sahu, A. K., Zaheer, M., Sanjabi, M., Talwalkar, A., and Smith, V. Federated optimization in heterogeneous networks. In *Proceedings of Machine learning and systems*, volume 2, pp. 429–450, 2020.
- Lian, X., Zhang, C., Zhang, H., Hsieh, C.-J., Zhang, W., and Liu, J. Can decentralized algorithms outperform centralized algorithms? a case study for decentralized parallel stochastic gradient descent. In *Advances in Neural Information Processing Systems*, pp. 5330–5340, 2017.
- Lin, Y., Han, S., Mao, H., Wang, Y., and Dally, W. J. Deep gradient compression: Reducing the communication bandwidth for distributed training. In *International Conference on Learning Representations*, 2018.
- Marfoq, O., Neglia, G., Bellet, A., Kameni, L., and Vidal, R. Decentralized federated learning: A survey and perspective. *IEEE Internet of Things Magazine*, 2023.
- McMahan, B., Moore, E., Ramage, D., Hampson, S., and y Arcas, B. A. Communication-efficient learning of deep networks from decentralized data. In *Artificial intelligence and statistics*, pp. 1273–1282. PMLR, 2017.
- Nesterov, Y. *Introductory Lectures on Convex Optimization: A Basic Course*, volume 87. Springer Science & Business Media, Boston, MA, 2004.
- Nesterov, Y. E. A method for solving the convex programming problem with convergence rate $O(1/k^2)$. *Soviet Mathematics Doklady*, 27(2):372–376, 1983.
- Philippenko, C. and Dieuleveut, A. A survey on decentralized federated learning. *arXiv preprint arXiv:2308.04604*, 2023.
- Polyak, B. T. Some methods of speeding up the convergence of iteration methods. *USSR Computational Mathematics and Mathematical Physics*, 4(5):1–17, 1964.
- Shi, Y., Feng, Y., Chen, W., Zhang, W., Ramamurthy, A., and Wilson, A. G. Personalized federated learning with gaussian processes. In *International Conference on Machine Learning*, pp. 19735–19753. PMLR, 2023.
- Sodiya, E. O., Umoga, U. J., Obaigbena, A., Jacks, B. S., Ugwuanyi, E. D., Daraojimba, A. I., and Lottu, O. A. Current state and prospects of edge computing within the internet of things (iot) ecosystem. *International Journal of Science and Research Archive*, 11(1):1863–1873, 2024. doi: 10.30574/ijrsra.2024.11.1.0287.
- Sun, Y., Zhou, S., and Gündüz, D. Collaborative learning on the edges: A case study on connected vehicles. In *2021 USENIX Annual Technical Conference*, pp. 635–648, 2021.
- Tan, A. Z., Yu, H., Cui, L., and Yang, Q. Survey of personalization techniques for federated learning. *arXiv preprint arXiv:2203.08568*, 2022.
- Thompson, G., Yue, K., Wong, C.-W., and Dai, H. NTK-DFL: Enhancing decentralized federated learning in heterogeneous settings via neural tangent kernel. In *Proceedings of the 42nd International Conference on Machine Learning*, pp. 267, Vancouver, Canada, 2025. PMLR. arXiv:2410.01922.
- Vogels, T., Karimireddy, S. P., and Jaggi, M. Powersgd: Practical low-rank gradient compression for distributed optimization. In *Advances in Neural Information Processing Systems*, volume 32, 2019.
- Xia, L., Liu, Z., Huang, S., Tang, W., and Liu, X. Non-linear trajectory modeling for multi-step gradient inversion attacks in federated learning. *arXiv preprint arXiv:2509.22082*, 2025. doi: 10.48550/arXiv.2509.22082. URL <https://arxiv.org/abs/2509.22082>.
- Xiao, H., Rasul, K., and Vollgraf, R. Fashion-MNIST: A novel image dataset for benchmarking machine learning algorithms, 2017.
- Yu, T., Song, C., Wang, J., and Chitnis, M. Momentum approximation in asynchronous private federated learning. *arXiv preprint arXiv:2402.09247*, 2024. Presented at International Workshop on Federated Foundation Models in Conjunction with NeurIPS 2024.
- Yu, Y., Khodak, M., Rawat, A. S., and Talwalkar, A. Tct: Convexifying federated learning using bootstrapped neural tangent kernels. In *Advances in Neural Information Processing Systems*, volume 35, pp. 23048–23061, 2022.
- Yue, K., Jin, R., Wong, C.-W., Baron, D., and Dai, H. Neural tangent kernel empowered federated learning. In *International Conference on Machine Learning*, pp. 25783–25803. PMLR, 2022.
- Zhang, C., Xie, Y., Bai, H., Yu, B., Li, W., and Gao, Y. A survey on federated learning. *Knowledge-Based Systems*, 216:106775, 2021.

Zhong, C. and Nie, X. A novel single-channel edge computing lora gateway for real-time confirmed messaging. *Scientific Reports*, 14(1):8369, 2024. doi: 10.1038/s41598-024-59058-8.

Zhu, J., Yao, R., and Blaschko, M. B. Surrogate model extension (sme): A fast and accurate weight update attack on federated learning. In *Proceedings of the 40th International Conference on Machine Learning, ICML '23*, pp. 43228–43257. PMLR, 2023.

Zhu, L., Liu, Z., and Han, S. Deep leakage from gradients. *Advances in neural information processing systems*, 32, 2019.